Echocardiographic evaluation of right ventricular diastolic function in pulmonary hypertension

Athiththan Yogeswaran [1,7], Zvonimir A. Rako[1,7], Selin Yildiz[1], Hossein Ardeschir Ghofrani [1], Werner Seeger [1], Bruno Brito da Rocha[1], Henning Gall [1], Nils C. Kremer[1], Philipp Douschan[1,2,3], Silvia Papa[4], Carmine Dario Vizza [4], Domenico Filomena[4], Ryan J. Tedford[5], Robert Naeije[6], Manuel J. Richter[1], Roberto Badagliacca[4,7] and Khodr Tello [1,7]

[1]Department of Internal Medicine, Justus-Liebig-University Giessen, Universities of Giessen and Marburg Lung Center (UGMLC), Member of the German Center for Lung Research (DZL), Giessen, Germany. [2]Department of Internal Medicine, Division of Pulmonology, Medical University of Graz, Graz, Austria. [3]Ludwig Boltzmann Institute for Lung Vascular Research, Graz, Austria. [4]Department of Clinical Internal, Anesthesiological and Cardiovascular Sciences, Sapienza University of Rome, Rome, Italy. [5]Division of Cardiology, Department of Medicine, Medical University of South Carolina, South Carolina, USA. [6]Free University of Brussels, Brussels, Belgium. [7]These authors contributed equally to this work.

Corresponding author: Khodr Tello (Khodr.Tello@innere.med.uni-giessen.de)

Shareable abstract (@ERSpublications)
This study introduces the echocardiographic peak lateral tricuspid annulus systolic velocity/right atrial area index ratio as a noninvasive measure of right ventricular diastolic function and predictor of prognosis in patients with pulmonary hypertension. https://bit.ly/44Qv8X0

Cite this article as: Yogeswaran A, Rako ZA, Yildiz S, *et al*. Echocardiographic evaluation of right ventricular diastolic function in pulmonary hypertension. *ERJ Open Res* 2023; 9: 00226-2023 [DOI: 10.1183/23120541.00226-2023].

Received: 7 April 2023
Accepted: 26 June 2023

Abstract

Background Right ventricular (RV) diastolic dysfunction may be prognostic in pulmonary hypertension (PH). However, its assessment is complex and relies on conductance catheterisation. We aimed to evaluate echocardiography-based parameters as surrogates of RV diastolic function, provide validation against the gold standard, end-diastolic elastance (Eed), and define the prognostic impact of echocardiography-derived RV diastolic dysfunction.

Methods Patients with suspected PH who underwent right heart catheterisation including conductance catheterisation were prospectively recruited. In this study population, an echocardiography-based RV diastolic function surrogate was derived. Survival analyses were performed in patients with precapillary PH in the Giessen PH Registry, with external validation in patients with pulmonary arterial hypertension at Sapienza University (Rome).

Results In the derivation cohort (n=61), the early/late diastolic tricuspid inflow velocity ratio (E/A) and early tricuspid inflow velocity/early diastolic tricuspid annular velocity ratio (E/e′) did not correlate with Eed ($p>0.05$). Receiver operating characteristic analysis revealed a large area under the curve (AUC) for the peak lateral tricuspid annulus systolic velocity/right atrial area index ratio (S′/RAAi) to detect elevated Eed (AUC 0.913, 95% confidence interval (CI) 0.839–0.986) and elevated end-diastolic pressure (AUC 0.848, 95% CI 0.699–0.998) with an optimal threshold of 0.81 $m^2 \cdot s^{-1} \cdot cm^{-1}$. Subgroup analyses demonstrated a large AUC in patients with preserved RV systolic function (AUC 0.963, 95% CI 0.882–1.000). Survival analyses confirmed the prognostic relevance of S′/RAAi in the Giessen PH Registry (n=225) and the external validation cohort (n=106).

Conclusions Our study demonstrates the usefulness of echocardiography-derived S′/RAAi for noninvasive assessment of RV diastolic function and prognosis in PH.

Introduction

Pulmonary hypertension (PH) is characterised by a chronic increase in right ventricular (RV) afterload resulting in impaired RV systolic function [1]. Accordingly, research has mainly focused on RV systolic function, and there are several invasive and noninvasive surrogates of RV contractility available and commonly applied [2–4]. However, increase of RV afterload leads – according to the LaPlace law – to meaningful hypertrophy and fibrosis, which in turn is one of the main contributors to stiffening of the

ventricle [5]. Furthermore, animal studies have shown that RV diastolic dysfunction might even be present before systolic RV failure occurs [6]. Consistent with this, it could be shown that patients with pulmonary arterial hypertension (PAH) have impaired RV diastolic function [7]. Further studies indicated that RV diastolic function is of crucial importance for both symptoms and survival not only in patients with right-sided heart failure but also in patients with left-sided heart failure [8–10]. Currently, it is hypothesised that the majority of patients with PH develop increased RV diastolic stiffness and dysfunction with mounting disease severity, resulting in vena cava backflow during atrial contraction due to impaired RV filling [5]. Early diagnosis of impaired RV diastolic function in PH is therefore crucial to prevent systemic complications and to reliably detect patients at risk, potentially supporting decision-making regarding escalation of therapy.

The gold-standard measure of RV diastolic function is end-diastolic elastance (Eed) derived from pressure–volume (PV) loops obtained by conductance catheterisation [11, 12]. However, conductance catheterisation is expensive, invasive and complex considering application and interpretation, and is consequently mainly restricted to expert centres [13]. So far, evidence regarding the use of standard imaging tools to assess RV diastolic dysfunction and its prognostic role is scarce. Tissue Doppler systolic and early diastolic velocities have shown promise in the left ventricle, correlating with fibrosis score and β-adrenergic receptor density in patients with left ventricular (LV) regional dysfunction [14]. However, commonly used parameters such as the ratio of early tricuspid inflow velocity to early diastolic tricuspid annular velocity (E/e′) and the ratio of early to late diastolic tricuspid inflow velocity (E/A) have not yet been validated for use as measures of RV diastolic dysfunction.

Speckle tracking echocardiography recently emerged as a potential tool allowing for the identification of phenotypically distinct, reproducible and clinically meaningful RV strain post-systolic patterns [15]. Recently, our group was able to define a noninvasive tool for the assessment of RV diastolic function using feature-tracking strain measurements from cardiac magnetic resonance imaging [16]. In the current study, we aimed to evaluate echocardiography-based parameters as potential surrogates of RV diastolic function, to provide validation against the gold standard, Eed, and to define the clinical and prognostic impact of echocardiography-derived RV diastolic dysfunction.

Methods

Study design and population

Prospectively, we recruited consecutive patients with clinically suspected PH undergoing right heart catheterisation including PV loop assessment (ClinicalTrials.gov: NCT04663217). Inclusion and exclusion criteria are summarised in supplementary table S1. Patients with atrial fibrillation at the time of right heart catheterisation or echocardiography were excluded from further analysis owing to the varying cardiac cycle length and consequently limited comparability.

For survival analyses, we included all patients with PAH or chronic thromboembolic PH (CTEPH) enrolled between 2008 and 2018 in the prospectively recruiting Giessen PH Registry if echocardiographic data (lateral tricuspid annulus peak systolic velocity (S′) and right atrial area (RAA)) were available within 12 months after/before diagnosis [17]. Patients without PAH or CTEPH were excluded from the survival analyses. All included patients were followed up until January 2022. Survival time was censored at 60 months after diagnosis.

The PH diagnosis was made by a multidisciplinary board (including physicians, radiologists and surgeons) according to the guidelines applicable at the time of diagnosis [18, 19].

RV diastolic dysfunction was defined as either Eed above the third quartile or end-diastolic pressure (EDP) above the third quartile. There is no universally accepted definition of RV diastolic dysfunction. The initial validation of E/e′ for the detection of LV diastolic dysfunction primarily relied on LV EDP [20]. However, from a haemodynamic perspective, it is important to consider the end-diastolic pressure–volume relationship, including the β coefficient and the calculation of Eed, along with EDP. We therefore incorporated both Eed and EDP in our definition of RV diastolic dysfunction.

The investigation conformed with the Declaration of Helsinki and was approved by the ethics committee of the Faculty of Medicine at the University of Giessen. All participating patients gave written informed consent.

Right heart catheterisation and PV loop assessment

Right heart catheterisation was performed as previously described [21]. PV loops were obtained using a PV catheter positioned in the RV apex, with the Inca PV Loop System (CD Leycom, Hengelo, The Netherlands)

for real-time visualisation (figure 1a). Eed was calculated offline as previously described [22]. In brief, Eed was calculated by a nonlinear fit of diastolic PV coordinates as $P=\alpha(e^{\beta V}-1)$ (where P is pressure, V is volume and α is a curve-fitting parameter) through the diastolic portion of the PV loops (figure 1a). For each patient, a mean Eed value was determined from three to five separate PV loops.

Echocardiography

Echocardiography was performed using a Philips Epiq 7G Elite (Philips Healthcare, Best, Netherlands) according to current guidelines for right heart imaging [23–25]. Using pulsed wave (tissue Doppler) echocardiography, S′ and tricuspid E, A and e′ were determined in the apical four-chamber view (figure 1b). RAA was measured at end-systole in an apical four-chamber view (figure 1b) and indexed for body surface area (RAAi) based on recommendations for assessment of LV diastolic function [26]. Body surface area was calculated as suggested by Du Bois and Du Bois [27].

Inter- and intra-observer variability was calculated from repeated measurements of S′ and RAA by two investigators unaware of the clinical data and diagnoses in a random subset of patients (n=15).

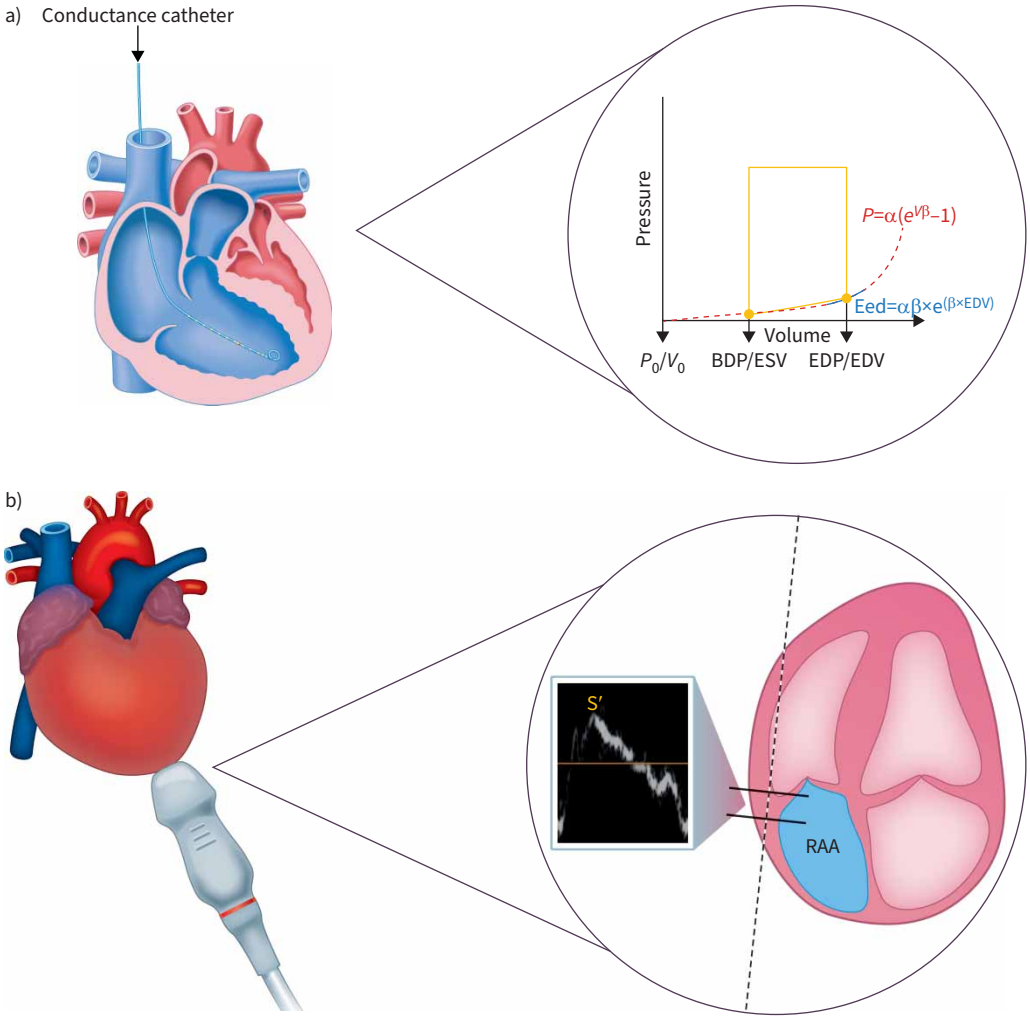

FIGURE 1 Evaluation of RV diastolic function. a) The gold-standard method for assessment of RV diastolic function is complex and invasive, requiring conductance catheterisation and calculation of Eed from pressure–volume loops. b) We evaluated the ratio of S′ to RAAi as a simple echocardiographic surrogate of RV diastolic function. α: curve fit parameter; BDP: beginning-diastolic pressure; EDP: end-diastolic pressure; EDV: end-diastolic volume; Eed: end-diastolic elastance; ESV: end-systolic volume; P: pressure; RAAi: right atrial area indexed to body surface area; RV: right ventricular; S′: lateral tricuspid annulus peak systolic velocity; V: volume.

External validation

External validation was performed in patients with PAH who underwent echocardiography at the Sapienza University of Rome.

Statistical analyses

Normality was assessed using the Shapiro–Wilk test ($p<0.05$ indicated non-normal distribution). Normal data are presented as mean±SD and non-normal data are presented as median (interquartile range) unless otherwise noted.

Differences between groups were assessed using chi-square tests for categorical data, t-tests for continuous normal data and Wilcoxon rank tests for continuous non-normal data. Spearman rho was used for correlation analyses.

Discriminatory power was determined by receiver operating characteristic (ROC) analysis using the R package *pROC*. As previously described, the Youden index was used to determine the optimal cut-off point [28].

Prognostic relevance was examined using univariate and multivariable Cox regression analyses. *A priori*, Schoenfeld residuals were assessed to confirm proportional hazard assumptions. The cut-off derived from the Youden index was used to classify patients into low and high RV myocardial stiffness groups. Survival was then compared between the two groups using Kaplan–Meier analyses and log-rank tests.

All analyses were performed with R Version 4.0 (The R Foundation, Vienna, Austria). $p<0.05$ was considered statistically significant.

Results

Baseline characteristics (prospective study cohort)

In total, 69 patients were screened in the prospective part of the study, of whom eight patients (12%) were excluded from further analysis owing to atrial fibrillation. Echocardiography was performed within 5 days before or after invasive diagnostics. Of the 61 included patients, 16 patients (26%) were diagnosed with PAH, five patients (8%) with PH due to left-sided heart disease (pulmonary venous hypertension) and 17 patients (28%) with CTEPH. In 23 cases (38%), PH was invasively ruled out by a mean pulmonary arterial pressure (mPAP) below 25 mmHg.

The median (IQR) age of the included patients was 66 (57–75) years and 40 patients (66%) were female. Median body mass index and mean body surface area were 29 (24–33) $kg \cdot m^{-2}$ and 1.4±0.3 m^2, respectively. Baseline echocardiography, right heart catheterisation and conductance data are shown in table 1. The intra-rater intraclass correlation coefficient was 0.967 for S′ and 0.976 for RAA. The inter-rater intraclass correlation coefficient was 0.882 for S′ and 0.940 for RAA.

Echocardiographic surrogates of RV myocardial stiffness

First, we investigated the correlation of echocardiographic surrogates of RV diastolic dysfunction (deduced from echocardiographic measures of LV diastolic function) with Eed and EDP (supplementary figure S1). Tricuspid E/A and E/e′ did not correlate with Eed ($p=0.49$ and $p=0.09$, respectively). Tricuspid E/e′ showed a moderate correlation with EDP (Spearman $\rho=0.38$, $p=0.003$), while tricuspid E/A did not correlate significantly with EDP ($p=0.74$).

We therefore introduced the S′/RAAi ratio as a surrogate marker of diastolic function and stiffness. S′ did not correlate with RAAi (Spearman $\rho=-0.06$, $p=0.65$) and multivariable linear backward regression including S′, RAAi, RV end-diastolic area (EDA), RV end-systolic area (ESA) and tricuspid E/A ratio showed that only S′ and RAAi were independently associated with Eed. In line with these associations, the S′/RAAi ratio correlated moderately with Eed (Spearman $\rho=-0.50$, $p<0.001$, figure 2a). In addition, S′/RAAi correlated with EDP (Spearman rho=−0.49, $p<0.001$; figure 2b), the minimum derivative of the change in diastolic pressure over time (dP/dt_{min}; Spearman $\rho=0.64$, $p<0.001$; figure 2c), RV ESA (Spearman $\rho=-0.62$, $p<0.001$) and RV EDA (Spearman $\rho=-0.51$, $p<0.001$).

A comparison of patients with precapillary PH (PAH or CTEPH) with the rest of the study population showed significantly increased Eed and EDP in the group with precapillary PH (figure 3a and 3b). Consistent with these findings, the S′/RAAi ratio was significantly decreased in the group with precapillary PH (figure 3c). Age and sex had no effect on Eed, EDP and the S′/RAAi ratio, as shown in supplementary figure S2. We performed sensitivity analyses in patients with mPAP ⩾25 mmHg (n=35). As in the overall

TABLE 1 Characteristics of derivation cohort

Parameter	All	S′/RAAi ratio <0.81 $m^2 \cdot s^{-1} \cdot cm^{-1}$	S′/RAAi ratio ⩾0.81 $m^2 \cdot s^{-1} \cdot cm^{-1}$	p-value
Patients	61 (100)	21 (34)	40 (66)	
Age years	66 (57–75)	67 (60–78)	65 (48–73)	0.16
Female	40 (66)	12 (57)	28 (70)	0.315
Body surface area m^2	1.4±0.3	1.2±0.3	1.5±0.3	0.004
NYHA FC				0.108
I	2 (3)	0 (0)	2 (5)	
II	16 (27)	3 (14)	13 (33)	
III	38 (63)	15 (71)	23 (59)	
IV	4 (7)	3 (14)	1 (3)	
Missing	1 (2)	0 (0)	1 (3)	
6MWD m	389 (304–445)	332 (279–382)	413 (354–450)	0.124
mPAP mmHg	28 (19–44)	48 (38–52)	22 (17–28)	<0.001
RAP mmHg	6 (5–9)	8 (5–11)	6 (5–7)	0.069
Cardiac index $L \cdot m^{-2}$	2.70 (2.28–3.14)	2.48 (2.11–2.77)	2.84 (2.47–3.23)	0.032
PCWP mmHg	10 (7–12)	9 (7–11)	11 (8–14)	0.135
PVR $dyn \cdot s \cdot cm^{-5}$	270 (136–553)	658 (522–783)	160 (114–286)	<0.001
IVC diameter mm	17.4±4.9	20.4±5.4	15.8±3.9	0.001
RAA cm^2	17 (13–22)	23 (20–33)	14 (12–17)	<0.001
RAAi $cm^2 \cdot m^{-2}$	12 (9–17)	19 (16–25)	10 (9–11)	<0.001
S′ $cm \cdot s^{-1}$	11.37±2.36	10.28±1.80	11.94±2.43	0.004
S′/RAAi ratio $m^2 \cdot s^{-1} \cdot cm^{-1}$	1.01±0.52	0.53±0.19	1.27±0.45	<0.001
RV EDA cm^2	25.1±7.9	30.4±7.1	22.3±6.8	<0.001
RV ESA cm^2	16.9±7.0	22.7±7.0	13.9±4.8	<0.001
RV FAC %	36 (25–44)	28 (16–33)	38 (30–44)	<0.001
TAPSE mm	22 (19–23)	19 (15–22)	22 (20–24)	0.002
TR severity				0.163
None	5 (8)	0	5 (13)	
Mild to moderate	48 (79)	18 (86)	30 (75)	
Severe	4 (7)	1 (5)	3 (8)	
Missing	4 (7)	2 (10)	2 (5)	
RV FWGLS %	−23±6	−20±7	−25±5	0.002
LV EF %	60±6	60±8	60±4	0.794
Eed $mmHg \cdot mL^{-1}$	0.169 (0.113–0.262)	0.274 (0.223–0.333)	0.143 (0.106–0.192)	<0.001
EDP mmHg	6 (3–9)	12 (6–15)	5 (2–7)	<0.001
Tau	34±10	41±7	31±10	<0.001

Data are presented as mean±SD, median (interquartile range) or n (%), unless otherwise stated. S′: lateral tricuspid annulus peak systolic velocity; RAAi: right atrial area indexed to body surface area; NYHA FC: New York Heart Association functional class; 6MWD: 6-min walk distance; mPAP: mean pulmonary arterial pressure; RAP: right atrial pressure; PCWP: pulmonary capillary wedge pressure; PVR: pulmonary vascular resistance; IVC: inferior vena cava; RAA: right atrial area; RV: right ventricular; EDA: end-diastolic area; ESA: end-systolic area; FAC: fractional area change; TAPSE: tricuspid annular plane systolic excursion; TR: tricuspid regurgitation; FWGLS: free wall global longitudinal strain; LV EF: left ventricular ejection fraction; Eed: end-diastolic elastance; EDP: end-diastolic pressure.

cohort, S′/RAAi correlated moderately with Eed (Spearman ρ=−0.61, p<0.001), EDP (Spearman ρ=−0.52, p=0.002) and dP/dt_{min} (Spearman ρ=0.50, p=0.005).

S′/RAAi ratio for detection of diastolic dysfunction

Next, we compared different echocardiographic surrogates in terms of their ability to detect diastolic dysfunction. Diastolic dysfunction was defined as either Eed above the third quartile (>0.262 $mmHg \cdot mL^{-1}$) or EDP above the third quartile (>9 mmHg).

ROC analysis revealed a small area under the ROC curve (AUC) of tricuspid E/A and tricuspid E/e′ for detection of high Eed (0.505, 95% confidence interval (CI) 0.372–0.636, and 0.665, 95% CI 0.529–0.783, respectively). However, the S′/RAAi ratio showed an AUC of 0.913 (95% CI 0.839–0.986) (figure 4a). The Youden index revealed that the optimal threshold of S′/RAAi indicating increased diastolic stiffness was 0.81 $m^2 \cdot s^{-1} \cdot cm^{-1}$. Sensitivity and specificity of S′/RAAi were 92% and 78%, respectively, resulting in a negative predictive value of 98% and accuracy of 85%.

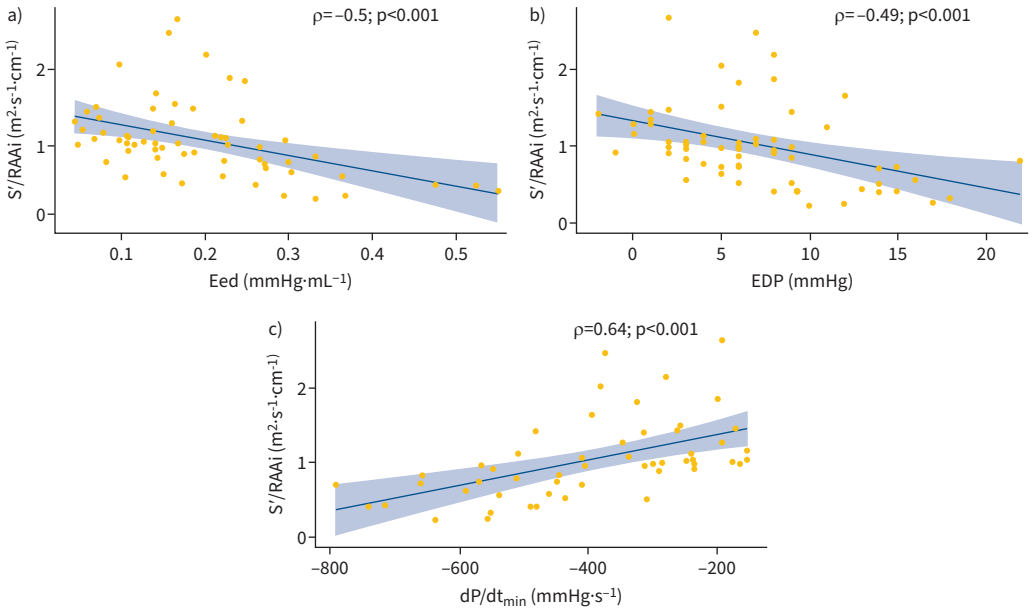

FIGURE 2 S′/RAAi correlation with measures of diastolic function. Correlations of S′/RAAi with a) Eed, b) EDP and c) dP/dt_{min} are shown. dP/dt_{min}: the minimum derivative of change in diastolic pressure over time; EDP: end-diastolic pressure; Eed: end-diastolic elastance; RAAi: right atrial area indexed to body surface area; S′: lateral tricuspid annulus peak systolic velocity.

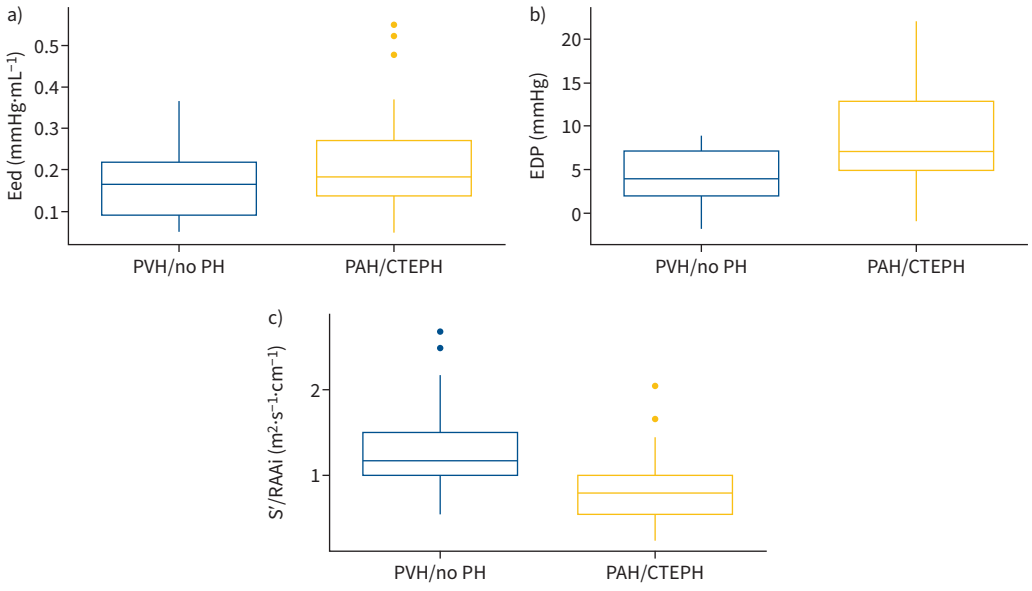

FIGURE 3 Diastolic function in precapillary PH (PAH/CTEPH) and PVH/no PH subgroups. Box and whisker plots are shown for a) Eed, b) EDP and c) S′/RAAi. Boxes show median and interquartile range; whiskers cover values within 1.5× the interquartile range above the third quartile or below the first quartile. Outliers are shown as individual data points. CTEPH: chronic thromboembolic pulmonary hypertension; EDP: end-diastolic pressure; Eed: end-diastolic elastance; PAH: pulmonary arterial hypertension; PH: pulmonary hypertension; PVH: pulmonary venous hypertension (pulmonary hypertension due to left-sided heart disease); RAAi: right atrial area indexed to body surface area; S′: lateral tricuspid annulus peak systolic velocity.

Consistent with this, direct comparison of tricuspid E/A, E/e′ and S′/RAAi ratios showed that S′/RAAi also had a substantially larger AUC for detection of diastolic dysfunction defined as EDP >9 mmHg (E/A: 0.525, 95% CI 0.323–0.727; E/e′: 0.750, 95% CI 0.612–0.888; S′/RAAi: 0.848, 95% CI 0.699–0.998; figure 4b). The optimal cut-off was again 0.81 $m^2 \cdot s^{-1} \cdot cm^{-1}$. Sensitivity, specificity and negative predictive values of S′/RAAi were 86%, 81% and 95%, respectively.

In addition, S′ and RAAi separately did not correlate as well as the new ratio with the gold standard, Eed (Spearman rho= −0.27, p=0.036 and Spearman rho=0.44, p<0.001, respectively). Correspondingly, the AUCs of S′ and RAAi for the detection of elevated Eed were smaller (0.686 (0.528–0.844) and 0.872 (0.759–0.986), respectively) than that of S′/RAAi.

In the prospective study population, a low S′/RAAi ratio (defined as S′/RAAi <0.81 $m^2 \cdot s^{-1} \cdot cm^{-1}$) was associated with increased mPAP and impaired cardiac index (table 1). Three-dimensional LV ejection fraction (EF), however, was not altered in patients with a low S′/RAAi ratio (60% *versus* 60%, p=0.79).

We performed a subgroup analysis in patients with mPAP >20 mmHg (the current definition of PH [29]; n=42). Even in this subgroup, S′/RAAi remained capable of distinguishing between patients with and without diastolic dysfunction defined either as Eed >0.262 $mmHg \cdot mL^{-1}$ (AUC 0.895, 95% CI 0.802–0.989) or as EDP >9 mmHg (AUC 0.829, 95% CI 0.673–0.985) (supplementary figure S3).

We also analysed the ratio of RV strain to RAAi in the whole prospective study population. RV strain/RAAi was able to distinguish diastolic dysfunction defined as Eed >0.262 $mmHg \cdot mL^{-1}$ (AUC 0.888, 95% CI 0.797–0.978) or EDP >9 mmHg (AUC 0.856, 95% CI 0.710–1.000) (supplementary figure S4).

S′/RAAi as a surrogate of diastolic RV function in patients with preserved systolic RV function

In a further analysis, we examined whether S′/RAAi is also associated with diastolic RV function in patients with preserved systolic RV function. Preserved RV systolic function was defined as 3D RV EF >50%, based on previous studies [30, 31]. Of the 21 relevant patients in our study population, three (14%) had an increased Eed. Notably, ROC analysis showed a large AUC (0.963 (0.882–1.000)) and high accuracy (95%) for the detection of RV diastolic dysfunction in patients with preserved RV systolic function.

Prognostic relevance of the S′/RAAi ratio in patients with precapillary PH

The prognostic significance of S′/RAAi was examined retrospectively in patients with PAH or CTEPH who were included in the Giessen PH Registry [17]. In total, 225 patients with available S′/RAAi were included in the survival analysis. The median time between the date of diagnosis and echocardiography

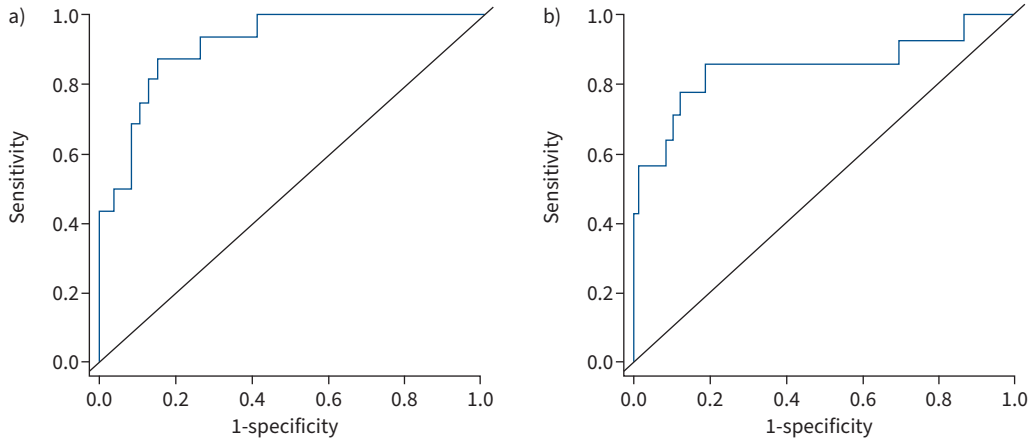

FIGURE 4 ROC analyses of S′/RAAi for detection of diastolic dysfunction. Diastolic dysfunction was defined as a) end-diastolic elastance above the third quartile (>0.262 $mmHg \cdot mL^{-1}$) and b) end-diastolic pressure above the third quartile (>9 mmHg). RAAi: right atrial area indexed to body surface area; ROC: receiver operating characteristic; S′: lateral tricuspid annulus peak systolic velocity.

was 4 (1–8) weeks. Baseline characteristics of the retrospective study cohort are shown in supplementary table S2.

Univariate Cox regression revealed an association of S′/RAAi (as a continuous variable) with mortality (hazard ratio (HR) 0.45, 95% CI 0.27–0.75), and an increased HR for mortality in patients with a low S′/RAAi ratio (HR 2.55, 95% CI 1.55–4.21; p<0.001). The concordance for the latter was 0.618±0.031 and the corresponding Schoenfeld plot is shown in supplementary figure S5. After adjustment for age and sex, the HR was 2.52 (95% CI 1.52–4.17; p<0.001). Accordingly, the Kaplan–Meier analysis showed significantly higher survival rates in patients with a high S′/RAAi ratio (defined as S′/RAAi $\geqslant$0.81 $m^2 \cdot s^{-1} \cdot cm^{-1}$) compared with those with a low S′/RAAi ratio (figure 5a; log-rank p<0.001). The 1-, 3- and 5-year survival rates were 93%, 85% and 80%, respectively, for patients with a high S′/RAAi ratio, and 75%, 61% and 57%, respectively, for patients with a low S′/RAAi ratio. Of note, the prognostic power of S′/RAAi was superior to those of tricuspid annular plane systolic excursion (TAPSE), pulmonary arterial systolic pressure (PASP), the TAPSE/PASP ratio, and pulmonary arterial acceleration time, as well as those of S′ and RAAi individually (supplementary table S3). Subgroup analysis in patients with PAH (n=117) showed that S′/RAAi is associated with prognosis in this subgroup of patients, as well as in the overall cohort (HR 2.77, 95% CI 1.54–4.98; p<0.001; Kaplan–Meier plot is shown in supplementary figure S6).

External validation was performed in a retrospective study cohort of 106 patients with PAH with a median age of 59 (50–70) years, of whom 28% were female. Baseline characteristics of the validation cohort are shown in supplementary table S4. Overall, 73 patients (69%) had a low S′/RAAi ratio indicating impaired diastolic function. Patients with a low S′/RAAi ratio were significantly older and had a significantly lower 6-min walk distance and higher New York Heart Association functional class than those with a high S′/RAAi ratio. Kaplan–Meier analysis revealed that survival of patients with a low S′/RAAi ratio was significantly impaired, compared with those with a high S′/RAAi ratio (figure 5b).

Discussion

Our study is the first to introduce and invasively validate the S′/RAAi ratio as an echocardiography-based surrogate parameter for RV diastolic function. The S′/RAAi ratio outperformed the currently used surrogates of RV diastolic stiffness and dysfunction in our study population and showed high discriminatory power for the detection of diastolic dysfunction as well as prognostic relevance.

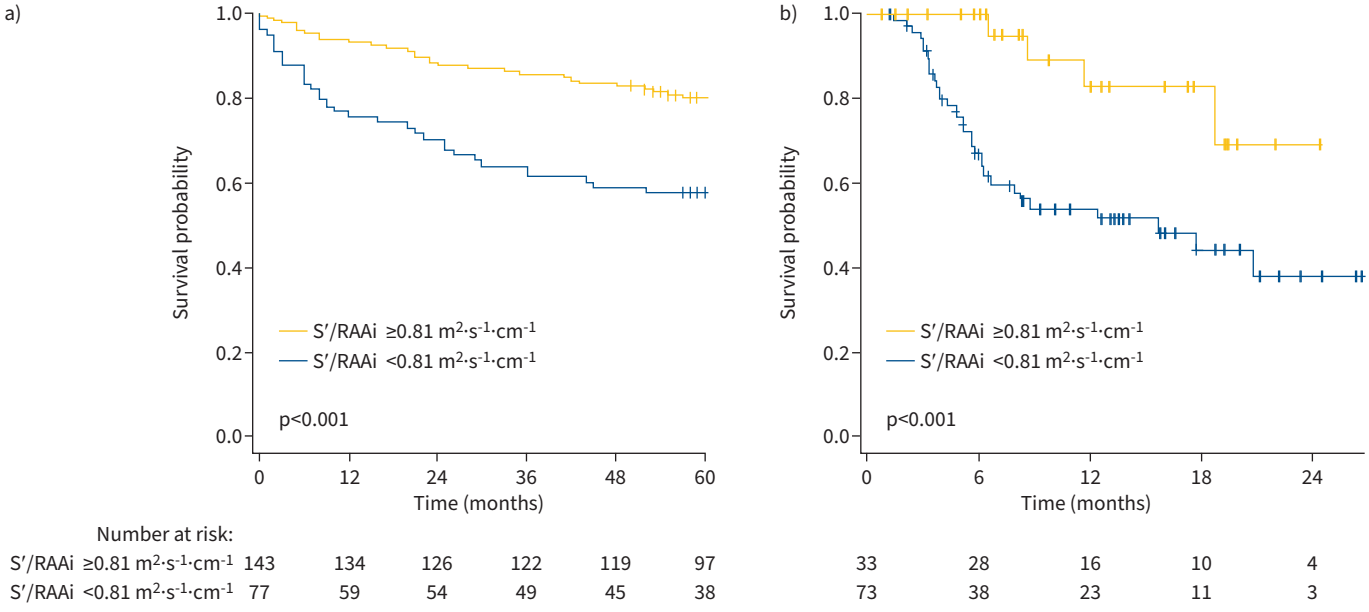

FIGURE 5 Association of the S′/RAAi ratio with survival in two independent cohorts of patients with PH. Kaplan–Meier analyses are shown for a) patients with PAH or chronic thromboembolic PH in the Giessen PH Registry (Germany) and b) patients with PAH at the University of Sapienza (Rome). PAH: pulmonary arterial hypertension; PH: pulmonary hypertension; RAAi: right atrial area indexed to body surface area; S′: lateral tricuspid annulus peak systolic velocity.

Importantly, the prognostic power of the S′/RAAi ratio was superior to that of the TAPSE/PASP ratio, which is widely acknowledged as a reliable prognostic parameter [4, 32] and is included in the current guidelines for risk assessment in PAH [29].

Diastolic dysfunction is caused by increased stiffness of myocardial sarcomeres due to decreased titin phosphorylation (among others) and/or enhanced interstitial fibrosis [7]. It results in increased RV diastolic filling pressure as the main reason for vena cava backflow during right atrial contraction [8]. Accordingly, vena cava backflow and subsequent end-organ damage are important prognostic biomarkers in patients with right heart insufficiency [8, 33]. However, it is crucial to detect patients at risk before congestion causes end-organ damage. Notably, in rats with monocrotaline-induced PH and in dogs with pulmonary artery banding, RV diastolic dysfunction was present even before RV systolic function was altered, highlighting the relevance of assessment of RV diastolic function [6, 34]. In patients with PH, RV diastolic stiffness is increased and associated with clinical worsening as well as prognosis [7, 11, 35]. Previous work by Vanderpool *et al.* [36] and Trip *et al.* [11] demonstrated the significance of RV diastolic dysfunction irrespective of RV systolic function, showing that RV–pulmonary arterial coupling alone cannot differentiate irreversible RV failure and non-response to treatment, whereas Eed provides discriminatory value. We employed Eed and EDP for the definition of RV diastolic dysfunction in our study to ensure that our analyses are sophisticated enough to define this complex phenotype appropriately.

In patients with left-sided heart failure, the mitral E/A and mitral E/e′ ratios are used to diagnose LV diastolic dysfunction [26]. We therefore evaluated whether their tricuspid equivalents (tricuspid E/A and tricuspid E/e′) correlate with gold-standard invasive parameters of RV diastolic function. Interestingly, despite their wide application, both tricuspid E/A and tricuspid E/e′ were not able to discriminate between preserved and impaired diastolic function.

Measurement of tissue Doppler-derived myocardial velocities has been commonly employed in recent decades. In 2000, a study showed that LV myocardial systolic velocity correlated strongly with interstitial fibrosis in patients with coronary artery disease who underwent transmural endomyocardial biopsy [14]. More recent studies showed alterations of LV myocardial systolic velocity in patients with metabolic syndrome and of S′ during simple aging [37, 38]. Again, LV myocardial systolic velocity was (indirectly) associated with fibrosis through its correlation with serum levels of transforming growth factor-β [38]. A recent study demonstrated that the stroke volume index/mitral S′ ratio may be superior to the mitral E/e′ ratio in assessing heart failure with preserved EF [39] and might serve as a parameter indicating diastolic dysfunction. Parameters widely used as measures of systolic function have been linked with impaired diastolic dysfunction [16]. Since increased myocardial stiffness and/or interstitial fibrosis are the main contributors to diastolic dysfunction, S′ may indeed be associated with RV diastolic function. Moreover, increased myocardial sarcomere stiffness and impaired diastolic filling of the right ventricle led to right atrial stress and eventual right atrial enlargement [8]. Right atrial function serves as a highly sensitive marker for changes in (diastolic) RV function, highlighting the importance of the right atrial–RV interaction. Notably, right atrial strain and RAAi have also been demonstrated to have prognostic relevance [40–44]. Altogether, these observations suggested a rationale for the utility of the ratio between S′ (as a marker of RV contractility, sarcomere function and fibrosis) and RAAi (as a marker for right atrial stress and increased RV diastolic filling pressure) for the detection of RV diastolic dysfunction. Although the RV strain/RAAi ratio was also able to discriminate diastolic dysfunction in our study, we chose not to utilise RV strain to ensure the simplicity and practicality of the chosen parameter.

In the present study, S′/RAAi showed appropriate correlations with PV loop-derived parameters of RV diastolic function including Eed as well as EDP and dP/dt_{min}. Notably, ROC analyses suggested that S′/RAAi can exclude diastolic dysfunction even in patients with preserved RV EF. S′ and RAAi, individually, did not perform as well as the new ratio for detecting RV diastolic dysfunction. Thus, S′/RAAi may be a new marker for RV diastolic (dys)function independent of RV systolic function. Further investigations in larger patient cohorts with preserved RV function, as defined by cardiac magnetic resonance imaging and/or 3D echocardiography, are needed to confirm this finding.

In a large cohort of patients with precapillary PH enrolled in the Giessen PH Registry as well as in an external validation cohort, S′/RAAi was associated with prognosis. Thus, S′/RAAi can be widely used for screening purposes as a surrogate marker of RV diastolic function. A high S′/RAAi ratio ($\geqslant 0.81\ m^2 \cdot s^{-1} \cdot cm^{-1}$) was able to exclude relevant RV diastolic dysfunction with high probability. Conversely, a low S′/RAAi ratio ($<0.81\ m^2 \cdot s^{-1} \cdot cm^{-1}$) is a warning signal for clinicians for the need of in-depth examination and possibly further invasive diagnostics including conductance catheterisation.

Furthermore, in the study subgroup of patients with preserved RV EF, up to 15% showed signs of diastolic dysfunction. Thus, the results of our study lead to the hypothesis that RV systolic dysfunction is closely linked to RV diastolic dysfunction, but that RV diastolic dysfunction precedes systolic dysfunction and can even be present in an isolated manner. This study is therefore the first to validate in humans the previously described, comparable observation first made in rats and dogs [6, 34].

Limitations of our study are the inclusion only of patients with (suspected) PH, the exclusion of patients with group 3 PH, and the delay of up to 5 days between invasive and noninvasive assessment of RV diastolic function. Data regarding the tricuspid regurgitation phenotype (atrial *versus* ventricular), which can influence RAAi, were not available in the derivation cohort. Small cohort size, outliers and heterogeneity of the study population may lead to a further bias. Thus, further studies are warranted to investigate whether S′/RAAi can be used to assess RV diastolic function in other cohorts, including patient populations with group 3 PH.

Taken together, our results provide evidence for the usefulness of the echocardiography-derived S′/RAAi ratio for the noninvasive evaluation of RV diastolic function and prognosis in patients with PH.

Provenance: Submitted article, peer reviewed.

Acknowledgements: Editorial assistance was provided by Claire Mulligan, PhD (Beacon Medical Communications Ltd, Brighton, UK), funded by the University of Giessen.

Data sharing statement: The datasets used and/or analysed during the current study are available from the corresponding author on reasonable request.

Author contributions: A. Yogeswaran, Z.A. Rako, R. Badagliacca and K. Tello conceived the idea for the analyses detailed in this manuscript. All authors contributed to the design and data collection in the study. A. Yogeswaran and H. Gall undertook statistical analyses of the data in the manuscript. All authors contributed to drafting and critical review of the manuscript. All authors approved the manuscript for submission.

Conflicts of interest: A. Yogeswaran reports non-financial support from the University of Giessen during the conduct of the study, and personal fees from MSD outside the submitted work. Z.A. Rako and N.C. Kremer report non-financial support from the University of Giessen during the conduct of the study. S. Yildiz has no conflict of interest or disclosures. H.A. Ghofrani reports grants from the German Research Foundation and non-financial support from the University of Giessen during the conduct of the study, and personal fees from Bayer, Actelion, Pfizer, Merck, GSK, and Takeda, grants and personal fees from Novartis, Bayer HealthCare, and Encysive/Pfizer, and grants from Aires, the German Research Foundation, Excellence Cluster Cardio-pulmonary Research, and the German Ministry for Education and research outside the submitted work. W. Seeger reports grants from the German Research Foundation and non-financial support from the University of Giessen during the conduct of the study, and personal fees from Pfizer and Bayer Pharma AG outside the submitted work. B. Brito da Rocha has no conflict of interest and nothing to disclose. H. Gall reports grants from the German Research Foundation and non-financial support from the University of Giessen during the conduct of the study, and personal fees from Actelion, AstraZeneca, Bayer, BMS, GSK, Janssen-Cilag, Lilly, MSD, Novartis, OMT, Pfizer, and United Therapeutics outside the submitted work. P. Douschan, S. Papa, C.D. Vizza and D. Filomena have no conflict of interest or disclosures. R.J. Tedford reports no direct conflicts of interest related to this manuscript; he reports general disclosures to include consulting relationships with Medtronic, Abbott, Aria CV Inc., Acceleron, Alleviant, CareDx, Cytokinetics, Itamar, Edwards LifeSciences, Eidos Therapeutics, Lexicon Pharmaceuticals, and Gradient. R.J. Tedford is the national principal investigator for the RIGHT-FLOW clinical trial (Edwards), serves on a steering committee for Merck and Abbott as well as a research advisory board for Abiomed. He also does hemodynamic core lab work for Merck. R. Naeije has relationships with drug companies including AOP Orphan Pharmaceuticals, Johnson & Johnson, Lung Biotechnology Corporation, and United Therapeutics. In addition to being an investigator in trials involving these companies, relationships include consultancy service, research grants, and membership of scientific advisory boards. M.J. Richter reports grants from the German Research Foundation and non-financial support from the University of Giessen during the conduct of the study, and personal fees from Actelion, Bayer, Janssen-Cilag, MSD, OMT, Pfizer, and United Therapeutics outside the submitted work. R. Badagliacca received grants and personal fees from Ferrer, Dompè, AOP, United Therapeutics, MSD, Janssen, and Bayer outside the submitted work. K. Tello reports grants from the German Research Foundation and non-financial support from the University of Giessen during the conduct of the study, and personal fees from Actelion outside the submitted work.

Support statement: This work was supported by the Excellence Cluster Cardio-Pulmonary System (ECCPS) and the Collaborative Research Center (SFB) 1213 - Pulmonary Hypertension and Cor Pulmonale, grant number SFB1213/1, project B08 (German Research Foundation, Bonn, Germany). Funding information for this article has been deposited with the Crossref Funder Registry.

References

1 Vonk Noordegraaf A, Chin KM, Haddad F, *et al.* Pathophysiology of the right ventricle and of the pulmonary circulation in pulmonary hypertension: an update. *Eur Respir J* 2019; 53: 1801900.
2 Richter MJ, Peters D, Ghofrani HA, *et al.* Evaluation and prognostic relevance of right ventricular-arterial coupling in pulmonary hypertension. *Am J Respir Crit Care Med* 2020; 201: 116–119.
3 Tello K, Axmann J, Ghofrani HA, *et al.* Relevance of the TAPSE/PASP ratio in pulmonary arterial hypertension. *Int J Cardiol* 2018; 266: 229–235.
4 Tello K, Wan J, Dalmer A, *et al.* Validation of the tricuspid annular plane systolic excursion/systolic pulmonary artery pressure ratio for the assessment of right ventricular-arterial coupling in severe pulmonary hypertension. *Circ Cardiovasc Imaging* 2019; 12: e009047.
5 Rako ZA, Kremer N, Yogeswaran A, *et al.* Adaptive versus maladaptive right ventricular remodelling. *ESC Heart Fail* 2023; 10: 762–775.
6 Gaynor SL, Maniar HS, Bloch JB, *et al.* Right atrial and ventricular adaptation to chronic right ventricular pressure overload. *Circulation* 2005; 112: Suppl. 9, I212–I218.
7 Rain S, Handoko ML, Trip P, *et al.* Right ventricular diastolic impairment in patients with pulmonary arterial hypertension. *Circulation* 2013; 128: 2016–2025.
8 Marcus JT, Westerhof BE, Groeneveldt JA, *et al.* Vena cava backflow and right ventricular stiffness in pulmonary arterial hypertension. *Eur Respir J* 2019; 54: 1900625.
9 Gan CT, Holverda S, Marcus JT, *et al.* Right ventricular diastolic dysfunction and the acute effects of sildenafil in pulmonary hypertension patients. *Chest* 2007; 132: 11–17.
10 Nagueh SF. Left ventricular diastolic function: understanding pathophysiology, diagnosis, and prognosis with echocardiography. *JACC Cardiovasc Imaging* 2020; 13: 228–244.
11 Trip P, Rain S, Handoko ML, *et al.* Clinical relevance of right ventricular diastolic stiffness in pulmonary hypertension. *Eur Respir J* 2015; 45: 1603–1612.
12 Vanderpool RR, Puri R, Osorio A, *et al.* EXPRESS: surfing the right ventricular pressure waveform: methods to assess global, systolic and diastolic RV function from a clinical right heart catheterization. *Pulm Circ* 2019; 10: 2045894019850993.
13 Tello K, Seeger W, Naeije R, *et al.* Right heart failure in pulmonary hypertension: diagnosis and new perspectives on vascular and direct right ventricular treatment. *Br J Pharmacol* 2021; 178: 90–107.
14 Shan K, Bick RJ, Poindexter BJ, *et al.* Relation of tissue Doppler derived myocardial velocities to myocardial structure and beta-adrenergic receptor density in humans. *J Am Coll Cardiol* 2000; 36: 891–896.
15 Badagliacca R, Pezzuto B, Papa S, *et al.* Right ventricular strain curve morphology and outcome in idiopathic pulmonary arterial hypertension. *JACC Cardiovasc Imaging* 2021; 14: 162–172.
16 Tello K, Dalmer A, Vanderpool R, *et al.* Cardiac magnetic resonance imaging-based right ventricular strain analysis for assessment of coupling and diastolic function in pulmonary hypertension. *JACC Cardiovasc Imaging* 2019; 12: 2155–2164.
17 Gall H, Felix JF, Schneck FK, *et al.* The Giessen Pulmonary Hypertension Registry: survival in pulmonary hypertension subgroups. *J Heart Lung Transplant* 2017; 36: 957–967.
18 Galie N, Hoeper MM, Humbert M, *et al.* Guidelines for the diagnosis and treatment of pulmonary hypertension: the Task Force for the Diagnosis and Treatment of Pulmonary Hypertension of the European Society of Cardiology (ESC) and the European Respiratory Society (ERS), endorsed by the International Society of Heart and Lung Transplantation (ISHLT). *Eur Heart J* 2009; 30: 2493–2537.
19 Galie N, Humbert M, Vachiery JL, *et al.* 2015 ESC/ERS Guidelines for the diagnosis and treatment of pulmonary hypertension: The Joint Task Force for the Diagnosis and Treatment of Pulmonary Hypertension of the European Society of Cardiology (ESC) and the European Respiratory Society (ERS): Endorsed by: Association for European Paediatric and Congenital Cardiology (AEPC), International Society for Heart and Lung Transplantation (ISHLT). *Eur Respir J* 2015; 46: 903–975.
20 Appleton CP, Hatle LK, Popp RL. Relation of transmitral flow velocity patterns to left ventricular diastolic function: new insights from a combined hemodynamic and Doppler echocardiographic study. *J Am Coll Cardiol* 1988; 12: 426–440.
21 Yogeswaran A, Richter MJ, Sommer N, *et al.* Evaluation of pulmonary hypertension by right heart catheterisation: does timing matter? *Eur Respir J* 2020; 56: 1901892.
22 Tello K, Richter MJ, Yogeswaran A, *et al.* Sex differences in right ventricular-pulmonary arterial coupling in pulmonary arterial hypertension. *Am J Respir Crit Care Med* 2020; 202: 1042–1046.

23 Lang RM, Badano LP, Mor-Avi V, *et al.* Recommendations for cardiac chamber quantification by echocardiography in adults: an update from the American Society of Echocardiography and the European Association of Cardiovascular Imaging. *J Am Soc Echocardiogr* 2015; 28: 1–39.e14.
24 Badano LP, Kolias TJ, Muraru D, *et al.* Standardization of left atrial, right ventricular, and right atrial deformation imaging using two-dimensional speckle tracking echocardiography: a consensus document of the EACVI/ASE/Industry Task Force to standardize deformation imaging. *Eur Heart J Cardiovasc Imaging* 2018; 19: 591–600.
25 Mitchell C, Rahko PS, Blauwet LA, *et al.* Guidelines for performing a comprehensive transthoracic echocardiographic examination in adults: recommendations from the American Society of Echocardiography. *J Am Soc Echocardiogr* 2019; 32: 1–64.
26 Nagueh SF, Smiseth OA, Appleton CP, *et al.* Recommendations for the evaluation of left ventricular diastolic function by echocardiography: an update from the American Society of Echocardiography and the European Association of Cardiovascular Imaging. *J Am Soc Echocardiogr* 2016; 29: 277–314.
27 Du Bois D, Du Bois EF. Clinical calorimetry: Tenth paper. A formula to estimate the approximate surface area if height and weight be known. *Arch Intern Med (Chic)* 1916; XVII: 863–871.
28 Gall H, Yogeswaran A, Fuge J, *et al.* Validity of echocardiographic tricuspid regurgitation gradient to screen for new definition of pulmonary hypertension. *EClinicalMedicine* 2021; 34: 100822.
29 Humbert M, Kovacs G, Hoeper MM, *et al.* 2022 ESC/ERS Guidelines for the diagnosis and treatment of pulmonary hypertension. *Eur Heart J* 2022; 43: 3618–3731.
30 Kovalova S, Necas J, Vespalec J. What is a “normal” right ventricle? *Eur J Echocardiogr* 2006; 7: 293–297.
31 Chua S, Levine RA, Yosefy C, *et al.* Assessment of right ventricular function by real-time three-dimensional echocardiography improves accuracy and decreases interobserver variability compared with conventional two-dimensional views. *Eur J Echocardiogr* 2009; 10: 619–624.
32 Fauvel C, Raitiere O, Boucly A, *et al.* Interest of TAPSE/sPAP ratio for noninvasive pulmonary arterial hypertension risk assessment. *J Heart Lung Transplant* 2022; 41: 1761–1772.
33 Yogeswaran A, Tello K, Lund J, *et al.* Risk assessment in pulmonary hypertension based on routinely measured laboratory parameters. *J Heart Lung Transplant* 2022; 41: 400–410.
34 Alaa M, Abdellatif M, Tavares-Silva M, *et al.* Right ventricular end-diastolic stiffness heralds right ventricular failure in monocrotaline-induced pulmonary hypertension. *Am J Physiol Heart Circ Physiol* 2016; 311: H1004–H1013.
35 Okumura K, Slorach C, Mroczek D, *et al.* Right ventricular diastolic performance in children with pulmonary arterial hypertension associated with congenital heart disease: correlation of echocardiographic parameters with invasive reference standards by high-fidelity micromanometer catheter. *Circ Cardiovasc Imaging* 2014; 7: 491–501.
36 Vanderpool RR, Hunter KS, Insel M, *et al.* The right ventricular-pulmonary arterial coupling and diastolic function response to therapy in pulmonary arterial hypertension. *Chest* 2022; 161: 1048–1059.
37 Innelli P, Esposito R, Olibet M, *et al.* The impact of ageing on right ventricular longitudinal function in healthy subjects: a pulsed tissue Doppler study. *Eur J Echocardiogr* 2009; 10: 491–498.
38 Sciarretta S, Ferrucci A, Ciavarella GM, *et al.* Markers of inflammation and fibrosis are related to cardiovascular damage in hypertensive patients with metabolic syndrome. *Am J Hypertens* 2007; 20: 784–791.
39 Mu G, Wang W, Liu C, *et al.* Combination of SVI/S’ and diagnostic scores for heart failure with preserved ejection fraction. *Clin Exp Pharmacol Physiol* 2023; 50: 677–687.
40 Alenezi F, Mandawat A, Il’Giovine ZJ, *et al.* Clinical utility and prognostic value of right atrial function in pulmonary hypertension. *Circ Cardiovasc Imaging* 2018; 11: e006984.
41 Fukuda Y, Tanaka H, Ryo-Koriyama K, *et al.* Comprehensive functional assessment of right-sided heart using speckle tracking strain for patients with pulmonary hypertension. *Echocardiography* 2016; 33: 1001–1008.
42 Richter MJ, Fortuni F, Alenezi F, *et al.* Imaging the right atrium in pulmonary hypertension: a systematic review and meta-analysis. *J Heart Lung Transplant* 2023; 42: 433–446.
43 Tello K, Dalmer A, Vanderpool R, *et al.* Right ventricular function correlates of right atrial strain in pulmonary hypertension: a combined cardiac magnetic resonance and conductance catheter study. *Am J Physiol Heart Circ Physiol* 2020; 318: H156–H164.
44 Wessels JN, Mouratoglou SA, van Wezenbeek J, *et al.* Right atrial function is associated with right ventricular diastolic stiffness: RA-RV interaction in pulmonary arterial hypertension. *Eur Respir J* 2022; 59: 2101454.